

## *N*-Aryl- and *N*-Thienylcarbazoles with Dimesitylboryl and 1,3,2-Benzodiazaborolyl Functions

Lothar Weber,<sup>\*,[a]</sup> Johannes Halama,<sup>[a]</sup> Lena Böhling,<sup>[a]</sup> Anna Chrostowska,<sup>\*,[b]</sup>  
Alain Dargelos,<sup>[b]</sup> Hans-Georg Stammler,<sup>[a]</sup> and Beate Neumann<sup>[a]</sup>

**Keywords:** Boron / Carbazoles / Density functional calculations / Photophysics

The reaction of the *N*-lithiated 3,6-di-*tert*-butylcarbazole with fluorodimesitylborene afforded the *N*-carbazolyl-functionalized dimesitylborene **1** as a colorless solid in 70 % yield. [4-(3,6-Di-*tert*-butylcarbazol-9-yl)phenyl]dimesitylborene (**2**) was synthesized in 59 % yield by the lithiation of *N*-(4-bromophenyl)-3,6-di-*tert*-butylcarbazole and the subsequent treatment of the organolithium compound with fluorodimesitylborene. Synthesis of yellow crystalline [5-(carbazol-9-yl)-2-thienyl]dimesitylborene **3** was effected in 66 % yield by the lithiation of 3,6-di-*tert*-butyl-*N*-(2-thienyl)carbazole and the subsequent reaction with fluorodimesitylborene. Coupling of *N*-(4-bromophenyl)-3,6-di-*tert*-butylcarbazole and 2-bromo-1,3-diethyl-1,3,2-benzodiazaborole with magnesium metal in

boiling THF in the presence of lithium chloride led to the formation of the functionalized benzodiazaborole **5** as a colorless solid in 68 % yield. Compounds **1–3** and **5** were characterized by elemental analyses, IR and NMR spectroscopy (<sup>1</sup>H, <sup>11</sup>B, <sup>13</sup>C) and mass spectrometry. The molecular structures of **1** and **3** were elucidated by X-ray diffraction analyses. The borylated systems show intense blue luminescence. The spectroscopic results were reproduced by TD-DFT calculations at the [B3LYP/6-311G(d,p)] level of theory. Thus, it was discovered that the LUMOs of **1–3** are located on the vacant 2p<sub>z</sub> orbital of the boron atom with contributions of the π\* orbital of the phenyl (in **2**) or thiophene (in **3**) unit, whereas the HOMOs are mainly represented by the carbazolyl unit.

### Introduction

Conjugated organic molecules and polymers containing three-coordinate boron have attracted considerable interest because of their optical and electronic properties, which make them potentially useful in functional materials.<sup>[1]</sup> Three-coordinate boron generally behaves as a π-acceptor due to its vacant p<sub>z</sub> orbital, which stabilizes the LUMO of an adjacent conjugated π-electron skeleton and thus lowers the HOMO–LUMO gap of these molecules. Thereby the dimesitylboryl (BMes<sub>2</sub>) function (Mes = 2,4,6-Me<sub>3</sub>C<sub>5</sub>H<sub>2</sub>) is the preferred substituent in which the coordinatively and electronically deficient boron center experiences the steric shielding of four *o*-methyl groups.<sup>[2–5]</sup> In the course of our studies on the chemical and physico-chemical properties of 1,3,2-diazaboroles and 1,3,2-benzodiazaboroles,<sup>[6]</sup> it was demonstrated that arenes, biphenyls, thiophenes, dithiophenes and arylalkynes functionalized by 1,3,2-benzodiazaborol-2-yl units exhibit intense blue luminescence upon UV irradiation with Stokes shifts up to 9500 cm<sup>−1</sup> and quantum efficiencies up to 0.99.<sup>[7–9]</sup> Our studies, however, have dis-

closed that the 1,3,2-benzodiazaborolyl group does not function as a π-acceptor as originally anticipated, but instead behaves as a π-donor substituent. The HOMOs of the molecules under investigation were mainly represented by the B/N heterocycle, whereas the LUMOs were located at the organic π-scaffold. Thus, the absorptions were explained by intramolecular charge-transfer processes. In keeping with this, the emission bands were subject to a pronounced solvatochromism.<sup>[8]</sup>

In a recent paper, we tried to design push–pull molecules in which the benzodiazaborolyl unit should be forced into the role of an acceptor by a carbazole as a prominent donor substituent at the other end of a π-system. To our surprise, the HOMO and LUMO of these species were both located on the carbazole part of the molecules, and the absorption spectrum showed transitions without the participation of the boron heterocycle.<sup>[10]</sup> In this context, it was interesting to replace the 1,3,2-benzodiazaborolyl moiety by the strongly π-accepting dimesitylboryl substituent and to study the photophysical behavior of the resulting molecules under otherwise comparable conditions.

[a] Fakultät für Chemie der Universität Bielefeld, 33615 Bielefeld, Germany  
E-mail: lothar.weber@uni-bielefeld.de

[b] Equipe Chimie Physique, IPREM, UMR 5254, Université de Pau et des Pays de l'Adour, 2 Av. du président Angot, B. P. 1155, 64013 Pau Cédex, France  
E-mail: anna.chrostowska@univ-pau.fr

Supporting information for this article is available on the WWW under <http://dx.doi.org/10.1002/ejic.201100123>.

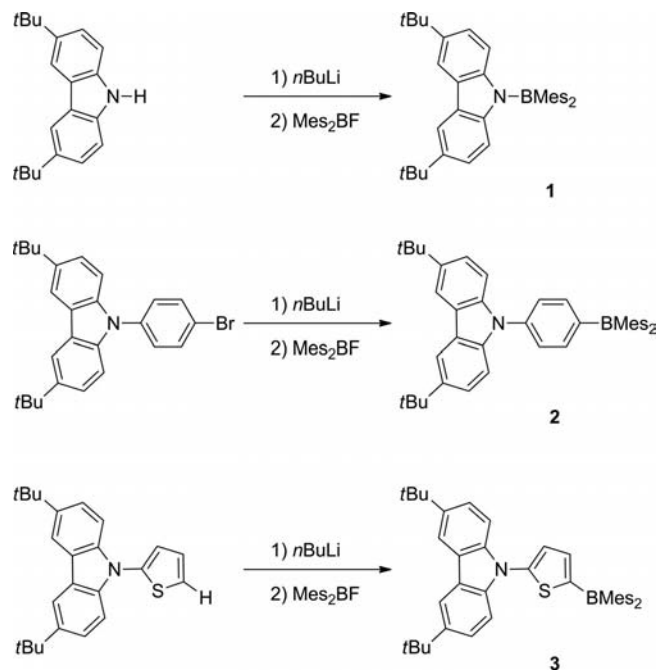
### Results and Discussion

The reaction of in situ generated *N*-lithiated 3,6-di-*tert*-butylcarbazole<sup>[11]</sup> with an equimolar amount of fluorodimesitylborene<sup>[12]</sup> in *n*-pentane at room temperature led to

the generation of the (carbazol-9-yl)dimesitylborane **1** as a colorless solid in 70% yield.

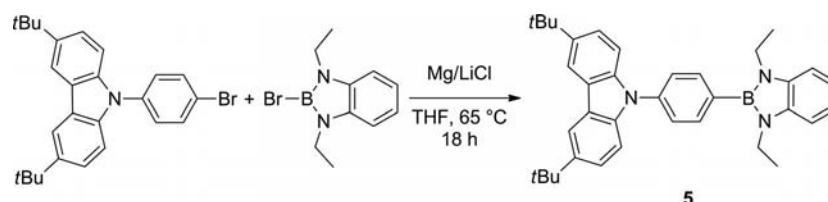
Lithiation of *N*-(4-bromophenyl)-3,6-di-*tert*-butylcarbazole was achieved by treatment with an equimolar amount of *n*-butyllithium in diethyl ether at  $-78^{\circ}\text{C}$ . After warming the mixture to  $-20^{\circ}\text{C}$ , a solution of fluorodimesitylborane in *n*-pentane was added. After hydrolysis, crude **2** was isolated from the organic layer and purified by crystallization from *n*-hexane. Pure **2** was obtained as colorless crystals in 59% yield.

The synthesis of [5-(carbazol-9-yl)-2-thienyl]dimesitylborane **3** was effected by the lithiation of 3,6-di-*tert*-butyl-*N*-(2-thienyl)carbazole<sup>[13]</sup> with *n*-butyllithium in diethyl ether at room temperature and the subsequent treatment of the resulting reaction mixture with an equivalent of fluorodimesitylborane. After the addition of water to the reaction mixture, yellow crystalline **3** was isolated by diethyl ether extraction, removal of volatile compounds from the extract, and crystallization of the residue from *n*-hexane at  $4^{\circ}\text{C}$  (66% yield) (Scheme 1).



Scheme 1. Syntheses of **1**–**3**.

For the validation of the capability of the dimesitylboryl and 1,3,2-benzodiazaborolyl groups as substituents on various luminescent carbazoles, the comparison of **1**–**3** with derivatives **4**–**6** is indispensable (Figure 1).



Scheme 2. Synthesis of **5**.

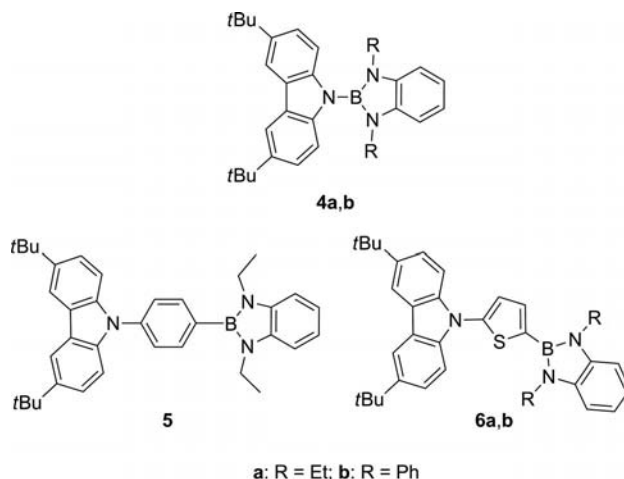


Figure 1. Compounds **4a,b**, **5** and **6a,b**.

Compounds **4a,b** and **6a,b** have been the subject of a recent paper.<sup>[10]</sup> The missing link, the 1,3,2-benzodiazaborole derivative **5**, was synthesized by the magnesium metal mediated coupling of equimolar quantities of 2-bromo-1,3-diethyl-1,3,2-benzodiazaborole and *N*-(4-bromophenyl)-3,6-di-*tert*-butylcarbazole<sup>[14]</sup> in boiling THF for 18 h (Scheme 2).

Compounds **1**–**3** are stable to oxygen and moisture, whereas **5** slowly decomposes when exposed to air. These new compounds are well soluble in common aprotic organic solvents. In the  $^{11}\text{B}\{^1\text{H}\}$ NMR spectrum of **1** a singlet was observed at  $\delta = 51.0$  ppm, whereas the respective singlet resonances of **2** and **3** are more deshielded ( $\delta = 64.9$  and  $71.3$  ppm, respectively). For benzodiazaborole **5**, an  $^{11}\text{B}\{^1\text{H}\}$ NMR resonance at  $\delta = 28.9$  ppm was observed.

### X-ray Structural Analysis of **1**

Single crystals of **1** suitable for an X-ray structural study (Table 5) were grown from an *n*-pentane solution at  $4^{\circ}\text{C}$ . The compound crystallizes in the monoclinic space group *C2/c*. The molecule (Figure 2) may be described as a dimesitylborane in which the third coordination site is occupied by a planar carbazole ring. The bond B(1)–N(1) [ $1.440(3)$  Å] is slightly shorter than the average B–N bond in the corresponding 2-(carbazol-9-yl)-1,3,2-benzodiazaborole **4a** [ $1.468(5)$  Å].<sup>[10]</sup> For the average B–N bond length in a sterically unhindered acyclic aminoborane, a value of  $1.41$  Å is given in the literature.<sup>[15]</sup> A particularly short B=N bond was measured in  $(\text{CF}_3)_2\text{B}=\text{N}i\text{Pr}_2$  [ $1.37(1)$  Å].<sup>[16]</sup>

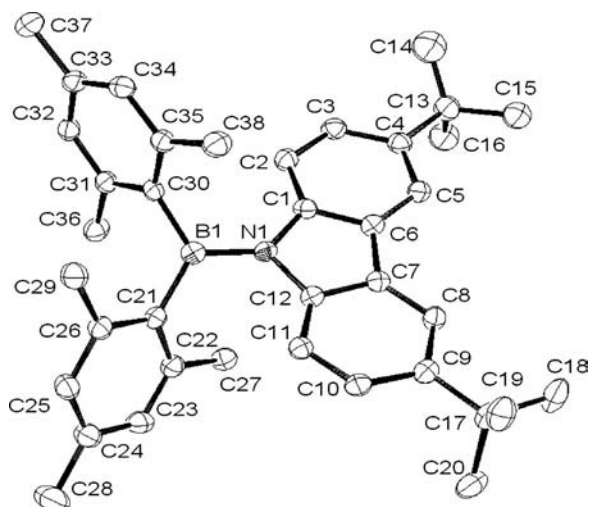


Figure 2. Molecular structure of **1**. Selected bond lengths [Å] and angles [°]: B(1)–N(1) 1.440(3), B(1)–C(21) 1.578(3), B(1)–C(30) 1.577(3), N(1)–C(1) 1.422(3), N(1)–C(12) 1.427(3), C(1)–C(6) 1.402(3), C(6)–C(7) 1.452(3), C(7)–C(12) 1.399(3), C(21)–C(22) 1.420(3), C(21)–C(26) 1.415(3), C(22)–C(23) 1.390(3), C(23)–C(24) 1.395(3), C(24)–C(25) 1.389(3), C(25)–C(26) 1.393(3), C(30)–C(31) 1.407(3), C(31)–C(32) 1.390(3), C(32)–C(33) 1.393(3), C(33)–C(34) 1.386(3), C(34)–C(35) 1.389(3), C(35)–C(30) 1.412(3); N(1)–B(1)–C(21) 119.6(2), C(21)–B(1)–C(30) 121.6(2), N(1)–B(1)–C(30) 118.8(2), B(1)–N(1)–C(1) 126.6(2), B(1)–N(1)–C(12) 127.6(2), C(1)–N(1)–C(12) 105.7(2), N(1)–C(1)–C(6) 110.0(2), C(1)–C(6)–C(7) 107.1(2), N(1)–C(12)–C(7) 110.2(2), C(6)–C(7)–C(12) 106.9(2); C(1)–N(1)–B(1)–C(21) 153.9, C(1)–N(1)–B(1)–C(30) –25.0, C(12)–N(1)–B(1)–C(21) –30.6, C(12)–N(1)–B(1)–C(30) 150.5.

Obviously, in **1** an optimal  $\pi$ -interaction between the  $2p_z$  orbitals at the boron atom and the carbazole part is prevented by the nonplanarity of the molecule. The plane of the carbazole and the plane defined by the N(1), C(30), and C(21) atoms enclose a dihedral angle of 28.2° and compares with the dihedral angles between the BC<sub>3</sub> planes and the fluorenyl plane (32.7° and 21.2°) in compound **7** (Figure 3).<sup>[17]</sup> These angles are markedly smaller than those between the NBC<sub>2</sub> plane and the mesityl rings in **1** (65.6° and 58.1°) and those between the BC<sub>3</sub> plane and the mesityl rings in **7** (51.8° and 54.9°). Mesityl relevant B–C bond lengths in **1** [B(1)–C(21) 1.578(3), B(1)–C(30) 1.577(3) Å] are well comparable to those in **7** [1.571(11)–1.592(10) Å], **8** [1.571(3), 1.581(3) Å] and **9** [1.573(3)–1.580(3) Å] (Figure 3).<sup>[18]</sup> Thus, molecule **1** is closer to planarity than the four conformers of the carbazole derivative **4a** (interplanar angles 55.9–77.7°; av. 66.6°).<sup>[10]</sup> For the N(1)–C(1) and

N(1)–C(12) distances [1.422(3), 1.427(3) Å], larger values were observed than in **4a** [1.402(5), 1.404(5) Å]. The C–C bond lengths within the five-membered ring in **1** [1.399(3), 1.402(3), 1.452(3) Å] are well comparable to those in **4a** [1.396(6), 1.407(5), 1.443(6) Å].

### X-ray Structural Analysis of **3**

Single crystals of **3** were grown from an *n*-hexane solution at 4 °C. The compound crystallizes in the monoclinic space group  $P2_1/c$ . The molecule (Figure 4) consists of a planar thiophene ring in which the 2-position is linked to the planar carbazole fragment by a single N(1)–C(21) bond [1.394(3) Å]. Both rings enclose an interplanar angle of 33.3°, which differs from the respective angle in **6a** (41.4°).

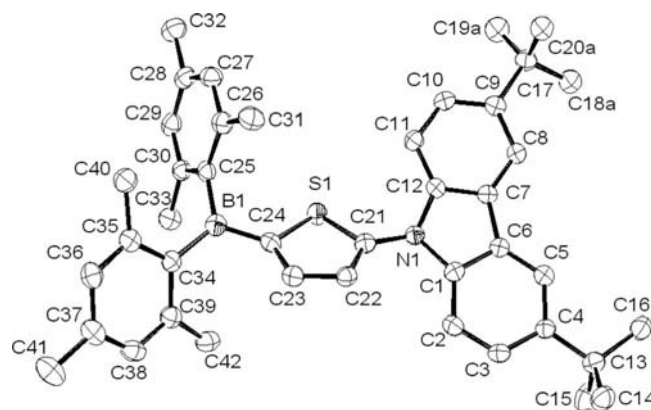


Figure 4. Molecular structure of **3**. Selected bond lengths [Å] and angles [°]: B(1)–C(24) 1.536(3), B(1)–C(25) 1.579(3), B(1)–C(34) 1.583(4), S(1)–C(24) 1.738(2), S(1)–C(21) 1.724(2), C(21)–C(22) 1.389(3), C(22)–C(23) 1.394(3), C(23)–C(24) 1.378(3), N(1)–C(21) 1.394(3), N(1)–C(1) 1.417(3), N(1)–C(12) 1.414(3), C(1)–C(6) 1.404(3), C(6)–C(7) 1.452(3), C(7)–C(12) 1.402(3), C(25)–C(26) 1.418(3), C(26)–C(27) 1.389(3), C(27)–C(28) 1.386(3), C(28)–C(29) 1.385(5), C(29)–C(30) 1.392(3), C(25)–C(30) 1.410(3), C(34)–C(35) 1.420(3), C(35)–C(36) 1.390(3), C(36)–C(37) 1.388(3), C(37)–C(38) 1.382(3), C(38)–C(39) 1.390(3), C(34)–C(39) 1.422(3); C(24)–B(1)–C(25) 117.8(2), C(24)–B(1)–C(34) 118.6(2), C(25)–B(1)–C(34) 123.5(2), B(1)–C(24)–S(1) 120.2(2), B(1)–C(24)–C(23) 130.2(2), C(21)–S(1)–C(24) 92.7(1), S(1)–C(21)–C(22) 110.8(2), C(21)–C(22)–C(23) 112.1(2), C(22)–C(23)–C(24) 115.3(2), S(1)–C(21)–N(1) 121.9(2), C(22)–C(21)–N(1) 127.3(2), C(21)–N(1)–C(1) 124.8(2), C(21)–N(1)–C(12) 126.7(2), C(1)–N(1)–C(12) 107.9(2), N(1)–C(1)–C(6) 108.7(2), C(1)–C(6)–C(7) 107.2(2), C(6)–C(7)–C(12) 107.5(2), N(1)–C(12)–C(7) 108.7(2); S(1)–C(24)–B(1)–C(25) –17.2, S(1)–C(24)–B(1)–C(34) 165.2, C(23)–C(24)–B(1)–C(34) –24.4, C(23)–C(24)–B(1)–C(25) 153.3, S(1)–C(21)–N(1)–C(12) 38.0, S(1)–C(21)–N(1)–C(1) –152.0, C(22)–C(21)–N(1)–C(12) –141.9, C(22)–C(21)–N(1)–C(1) 28.1.

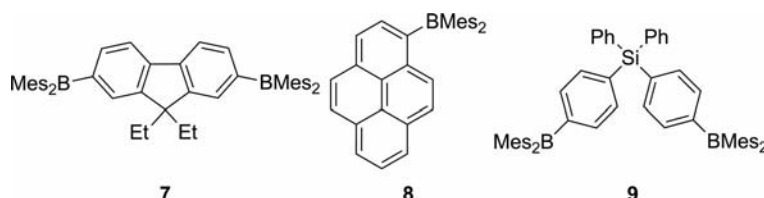


Figure 3. Compounds **7**–**9**.

In the 5-position, the thiophene ring is attached to a dimesitylboryl group by a B(1)–C(14) single bond [1.536(3) Å]. For comparison, the B–C(thiophene) bond in **6a** was found to be slightly longer [1.557(2) Å]. Mesityl relevant B–C bond lengths in **3** are in the expected range [B(1)–C(25) 1.579(3), B(1)–C(34) 1.583(4) Å]. The plane defined by the C(24), C(25), and C(34) atoms, including the boron atom, is twisted out of the plane of the thiophene ring by 21.8°. The interplanar angles between this plane and the mesityl groups are 64.4° and 48.3°. Bond angles and bond lengths within the carbazole part of **3** are similar to those of compound **1**. In summary, molecule **3** is closer to planarity than the diazaborolyl analog **6a**. This observation and the shorter B–C(thiophene) bonds point an increased  $\pi$ -communication within **3**.

### UV/Vis and Luminescence Spectra

Table 1 lists selected photophysical data for compounds **1–3**, all of which exhibit intense blue luminescence under UV irradiation. For comparison, the photophysical data for the analogous systems with the 1,3,2-benzodiazaborolyl function **4a,b**, **5** and **6a,b** are also included.

As reported previously, the UV/Vis spectrum of 3,6-di-*tert*-butylcarbazole (in cyclohexane) is dominated by a strong absorption band at  $\lambda = 296$  nm ( $\epsilon = 18114$  L mol<sup>−1</sup> cm<sup>−1</sup>) and a significantly weaker band at  $\lambda = 337$  nm ( $\epsilon = 2672$  L mol<sup>−1</sup> cm<sup>−1</sup>). In line with theoretical calculations, the band at  $\lambda = 296$  nm was assigned to a transition from the HOMO–1 into the LUMO of the molecule, whereas that at  $\lambda = 337$  nm reflects the HOMO–LUMO transition.<sup>[10]</sup> In the UV/Vis spectrum of **1** (in cyclohexane), an intense band was observed at  $\lambda = 288$  nm ( $\epsilon = 21800$  L mol<sup>−1</sup> cm<sup>−1</sup>) in addition to a less intense band at  $\lambda = 324$  nm ( $\epsilon = 14072$  L mol<sup>−1</sup> cm<sup>−1</sup>). The high intensity of the latter band may indicate the superposition of a CT band and a transition within the carbazole system. The positions of these absorptions are virtually the same for THF or CH<sub>2</sub>Cl<sub>2</sub> solutions of **1**. The absence of solvatochromism points to a low dipole moment of the compound in the ground state ( $\mu_{\text{g,calc.}} = 0.21$  D). In the luminescence spectrum of **1** (in cyclohexane), a strong band was observed at  $\lambda = 450$  nm (Stokes shift 9000 cm<sup>−1</sup>), which in a THF or CH<sub>2</sub>Cl<sub>2</sub> solution is redshifted to 479 (Stokes shift 10200 cm<sup>−1</sup>) or 492 nm (10700 cm<sup>−1</sup>), respectively. The large Stokes shifts and the solvatochromism are consistent with a more polar excited state resulting from an intramolecular charge transfer ( $\mu_{\text{g,calc.}} = 3.70$  D).

This clearly contrasts with the photophysical behavior of the 2-(carbazol-9-yl)-1,3,2-benzodiazaboroles **4a,b** in which Stokes shifts of only 500–700 cm<sup>−1</sup> (in cyclohexane) were observed. The virtual absence of solvatochromism was confirmed by quantum-chemical calculations, which point to electronic transitions within the carbazole fragment without the participation of the B/N heterocycle. Thus, no significant dipole moment of the molecule was present in the excited state.<sup>[10]</sup>

The formal insertion of a phenylene unit into the B–N bond of **1** provides an elongated  $\pi$ -electron scaffold for molecule **2**. The cyclohexane solution of **2** displays three absorptions in the UV/Vis spectrum at  $\lambda = 296$  ( $\epsilon = 16364$ ), 330 (9494), and 374 nm (18120 L mol<sup>−1</sup> cm<sup>−1</sup>). The CT band at lowest energy, which reflects the HOMO–LUMO transition, experiences a redshift of 50 nm compared with **1**. In the related compound **10** (Figure 5), the corresponding CT band was observed at 362 nm.<sup>[19]</sup> The bands at  $\lambda = 330$  and 296 nm are tentatively assigned to the carbazole-centered HOMO  $\rightarrow$  LUMO+1 and HOMO–1  $\rightarrow$  LUMO+1 transitions, respectively.

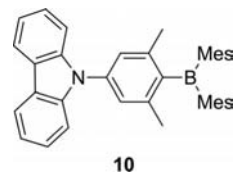


Figure 5. Compound **10**.

The CT absorption band in **2** shows a slight negative solvatochromism with  $\lambda_{\text{max}} = 367$  (THF) and 363 nm (CH<sub>2</sub>Cl<sub>2</sub>). Such negative solvatochromic behavior was also reported for **10** and other acceptor-substituted carbazoles<sup>[20,21]</sup> and is most likely due to a dipole inversion upon S<sub>0</sub> $\rightarrow$ S<sub>1</sub> excitation. In the absence of effective  $\pi$ -conjugation, the ground-state polarization of **2** is essentially determined by inductive effects with the boron atom as a  $\sigma$ -donor and the nitrogen atom as  $\sigma$ -acceptor ( $\mu_{\text{g,calc.}} = 0.83$  D). Upon excitation of **2**, the direction of the dipole-moment vector reverses, because charge is transferred from the nitrogen atom to the boron atom. Thus, the solvent molecules have an energetically unfavorable orientation and need to be reorganized at the expense of energy, particularly in polar media. In contrast, the emission band of **2** shows the expected positive solvatochromism. Bands in the luminescence spectra at  $\lambda = 394$  (cyclohexane), 452 (THF), and 461 nm (CH<sub>2</sub>Cl<sub>2</sub>) with Stokes shifts of 1400 (cyclohexane), 5400 (THF) and 6100 cm<sup>−1</sup> (CH<sub>2</sub>Cl<sub>2</sub>) are diagnostic for a polar excited state of **2** ( $\mu_{\text{g,calc.}} = 12.61$  D). The quantum efficiencies are quite high ( $\Phi = 0.78$  in cyclohexane, 0.77 in THF, 0.70 in CH<sub>2</sub>Cl<sub>2</sub>). Derivative **10** gave rise to blue emission at  $\lambda = 387$  nm with a quantum yield of  $\Phi = 0.62$  and a Stokes shift of 1800 cm<sup>−1</sup> in cyclohexane.<sup>[19]</sup>

In compound **5**, which is derived from **2** by the replacement of the dimesitylboryl group by the 1,3-diethyl-1,3,2-benzodiazaborolyl unit, UV/Vis absorption bands were observed in cyclohexane, THF and CH<sub>2</sub>Cl<sub>2</sub> at  $\lambda = 298$  and 329 nm. Again, the band at lower energy is assigned to the HOMO–LUMO and the second band to a HOMO–1  $\rightarrow$  LUMO transition; the absence of solvatochromism is obvious.

The fluorescence spectrum of **2** shows a positive solvatochromism with bands at  $\lambda = 366$  (cyclohexane), 370 (THF), and 372 nm (CH<sub>2</sub>Cl<sub>2</sub>). Markedly, larger Stokes shifts of 3200 (cyclohexane) to 3600 cm<sup>−1</sup> (CH<sub>2</sub>Cl<sub>2</sub>) may be explained by an extensive reorganization of the structure of **5** in the excited state.



Table 1. Selected photophysical data of compounds **1–3**, **4a,b**, **5**, and **6a,b**.

Compound	$\lambda_{\text{max,abs}}$ [nm]	$\lambda_{\text{max,abs}}$ [cm <sup>-1</sup> ]	$\epsilon$ [Lmol <sup>-1</sup> cm <sup>-1</sup> ]	$\lambda_{\text{max,em}}$ [nm]	$\lambda_{\text{max,em}}$ [cm <sup>-1</sup> ]	Stokes shift [cm <sup>-1</sup> ]	$\Phi_{\text{f}}^{[d]}$
<b>1</b> <sup>[a]</sup>	288	34700	21800				
	324	30900	14072	450	21900	9000	0.15
<b>1</b> <sup>[b]</sup>	288	34700	18553				
	325	30800	12209	479	20600	10200	0.19
<b>1</b> <sup>[c]</sup>	288	34700	16720				
	325	30800	11030	492	20100	10700	0.31
<b>2</b> <sup>[a]</sup>	296	33800	16364				
	330	30300	9494				
	374	26700	18120	394	25300	1400	0.78
<b>2</b> <sup>[b]</sup>	296	33800	21049				
	333	30000	13255				
	367	27200	22111	452	21800	5400	0.77
<b>2</b> <sup>[c]</sup>	297	33700	11433				
	335	29900	7552				
	363	27500	11977	461	21400	6100	0.70
<b>3</b> <sup>[a]</sup>	295	33900	18256				
	327	30600	10858				
	390	25600	25663	414	24000	1600	0.43
<b>3</b> <sup>[b]</sup>	294	34000	20663				
	327	30600	11253				
	390	25600	25472	445	22300	3300	0.41
<b>3</b> <sup>[c]</sup>	295	33900	16443				
	327	30600	9397				
	387	25800	8427	452	21900	3900	0.32
<b>4a</b> <sup>[a]</sup>	297	33700	16676				
	340	29400	2643	345	29900	500	0.37
<b>4a</b> <sup>[b]</sup>	296	33800	23080				
	340	29400	4251	348	28700	700	0.09
<b>4a</b> <sup>[c]</sup>	296	33800	17990				
	341	29300	2900	349	28600	700	0.44
<b>4b</b> <sup>[a]</sup>	296	33800	17336				
	335	29800	1532	342	29100	700	0.41
<b>4b</b> <sup>[b]</sup>	297	33700	15895				
	336	29800	3149	344	29000	800	0.33
<b>4b</b> <sup>[c]</sup>	296	33700	19945				
	337	30800	3329	346	28800	2000	0.46
<b>5</b> <sup>[a]</sup>	298	33600	31650				
	329	30400	6580	366	27200	3200	0.48
<b>5</b> <sup>[b]</sup>	298	33600	15023				
	329	30400	5389	370	26900	3500	0.40
<b>5</b> <sup>[c]</sup>	298	33600	17662				
	329	30400	5292	372	26800	3600	0.40
<b>6a</b> <sup>[a]</sup>	296	33800	14488				
	321	31100	9509	371	25800	5300	0.14
<b>6a</b> <sup>[b]</sup>	296	33800	13661				
	323	31000	9509	389	25200	5800	0.15
<b>6a</b> <sup>[c]</sup>	297	33700	22780				
	320	31300	15760	395	25000	6300	0.21
<b>6b</b> <sup>[a]</sup>	296	33800	22628				
	328	30500	9931	386	25500	5000	0.13
<b>6b</b> <sup>[b]</sup>	296	33800	28555				
	330	30300	13194	388	25300	5000	0.15
<b>6b</b> <sup>[c]</sup>	297	33700	15380				0.18
	330	30300	10710	396	25000	5300	

[a] In cyclohexane. [b] In THF. [c] In CH<sub>2</sub>Cl<sub>2</sub>. [d] Against standard POPOP ( $\Phi = 0.93$ ).

The UV/Vis spectrum of **3** in cyclohexane is characterized by bands at  $\lambda = 295$  nm ( $\epsilon = 18256$ ), 327 (10858), and 390 nm (25663 Lmol<sup>-1</sup> cm<sup>-1</sup>). In THF and CH<sub>2</sub>Cl<sub>2</sub> solutions of **3**, no significant shifts of these absorptions are noted. Accordingly, the ground-state dipole moment is calculated as  $\mu_{\text{g,calcd.}} = 0.21$  D. The CT band with the lowest energy is attributed to the HOMO–LUMO transition. In

comparison with **2**, this absorption band is redshifted by  $\lambda = 26$  nm; for the corresponding 1,3,2-benzodiazaborole derivative **6a**, this band is redshifted by  $\lambda = 69$  nm. In the luminescence spectrum of **3** in cyclohexane, a band at  $\lambda = 414$  nm is observed, which is redshifted in THF and CH<sub>2</sub>Cl<sub>2</sub> to  $\lambda = 445$  and 452 nm, respectively. The increased polarity of the excited state was confirmed computationally by a

dipole moment of  $\mu_{\text{g,calcd.}} = 9.93$  D. These data correspond to Stokes shifts of 1600 (cyclohexane), 3300 (THF), and 3900  $\text{cm}^{-1}$  ( $\text{CH}_2\text{Cl}_2$ ).

In the UV/Vis spectrum of 2-[5-(carbazol-9-yl)-2-thienyl]-1,3-diethyl-1,3,2-benzodiazaborole **6a**, absorption bands in cyclohexane were encountered at  $\lambda = 296$  ( $\epsilon = 14488$ ) and 321 nm ( $9509 \text{ L mol}^{-1} \text{ cm}^{-1}$ ). The luminescence spectrum of **6a** was characterized by intense emissions at  $\lambda = 371$  (cyclohexane), 389 (THF), and 395 nm ( $\text{CH}_2\text{Cl}_2$ ), combined with Stokes shifts of 5300, 5800, and 6300  $\text{cm}^{-1}$ , respectively. The larger Stokes shifts in **6a** compared with **3** underlines that, in the ground state, molecule **3**, with only two linked-ring systems, is closer to planarity than the diazaborole analogue **6a**. This finding and the shorter B–C(thiophene) bonds point to an increased  $\pi$ -communication within **3**.

### DFT Calculations

Table 2 contains selected [CAM-B3LYP/6-311G(d,p)] calculated geometrical parameters for **1** and **3** in addition to their experimental structural data.

For compound **1**, the experimentally determined bond lengths and valence angles (Table 2) are not essentially different from those calculated, with the exception of the C(21)–C(22) and C(30)–C(35) bond lengths for which the calculated value 1.391 Å is slightly shorter than the experimental ones [1.420(3) and 1.407(3) Å]. The same holds for the C(21)–B(1)–C(30) angle [calcd. 120.2°; exp. 121.6(2)°]. In contrast to this, the calculated value for the C(30)–B(1)–N(1) angle (119.9°) is slightly more obtuse than the experimentally determined one [118.8(2)°]. The calculated value of the N–C bond length in the carbazole (1.386 Å) increases marginally from 1.401 Å [exp. av. 1.403(5) Å] in **6a** to 1.420 Å [exp. av. 1.425(3) Å] in **1**.

The calculated absorption maxima from TD-DFT computations, carried out on the optimized geometries of **1–3**, and the corresponding oscillator strengths  $f$  are displayed in Table 3. The calculation for **1** gave a lowest energy band at  $\lambda = 288$  nm for an allowed  $S_0 \rightarrow S_1$  electronic absorption with an oscillator strength  $f = 0.31$ , which corresponds to the HOMO  $\rightarrow$  LUMO transition. This calculated value differs from the observed absorption maximum at  $\lambda = 324$  nm by 36 nm. The redshift may be due to the fact that in solu-

Table 2. Selected experimental and calculated [CAM-B3LYP/6-311G(d,p)] bond lengths [Å] and angles [°] for **1** and **3**.

	<b>1</b> calcd.	<b>1</b> exp.		<b>3</b> calcd.	<b>3</b> exp.
B(1)–N(1)	1.438	1.440(3)	B(1)–C(24)	1.542	1.536(3)
B(1)–C(21)	1.580	1.578(3)	B(1)–C(25)	1.579	1.579(3)
B(1)–C(30)	1.580	1.577(3)	B(1)–C(34)	1.580	1.583(4)
C(21)–C(26)	1.409	1.415(3)	S(1)–C(24)	1.741	1.738(2)
C(21)–C(22)	1.391	1.420(3)	S(1)–C(21)	1.731	1.724(2)
C(30)–C(31)	1.391	1.407(3)	C(21)–C(22)	1.369	1.389(3)
C(30)–C(35)	1.409	1.412(3)	C(22)–C(23)	1.410	1.394(3)
N(1)–C(12)	1.420	1.427(3)	C(23)–C(24)	1.376	1.378(3)
N(1)–C(1)	1.420	1.422(3)	N(1)–C(21)	1.393	1.394(3)
C(12)–C(11)	1.392	1.395(3)	N(1)–C(12)	1.399	1.414(3)
C(12)–C(7)	1.398	1.399(3)	N(1)–C(1)	1.399	1.417(3)
C(1)–C(12)	1.392	1.390(3)	C(12)–C(7)	1.401	1.402(3)
C(1)–C(6)	1.398	1.402(3)	C(1)–C(6)	1.401	1.404(3)
C(6)–C(7)	1.448	1.452(3)	C(6)–C(7)	1.449	1.452(3)
C(21)–B(1)–N(1)	119.9	119.6(2)	C(24)–B(1)–C(25)	119.4	117.8(2)
C(30)–B(1)–N(1)	119.9	118.8(2)	C(24)–B(1)–C(34)	117.4	118.6(2)
C(21)–B(1)–C(30)	120.2	121.6(2)	C(25)–B(1)–C(34)	123.2	123.5(2)
B(1)–N(1)–C(12)	127.1	127.6(2)	B(1)–C(24)–S(1)	122.5	120.2(2)
B(1)–N(1)–C(1)	127.1	126.6(2)	B(1)–C(24)–C(23)	128.0	130.2(2)
C(1)–N(1)–C(12)	105.8	105.7(2)	C(21)–S(1)–C(24)	92.1	92.7(1)
N(1)–C(1)–C(6)	110.1	110.0(2)	S(1)–C(21)–C(22)	111.5	110.8(2)
C(1)–C(6)–C(7)	107.0	107.1(2)	S(1)–C(21)–N(1)	121.8	121.9(2)
C(2)–C(1)–C(6)	119.6	119.8(2)	N(1)–C(12)–C(7)	109.1	108.7(2)
C(1)–N(1)–B(1)–C(21)	154.2	153.9			
C(12)–N(1)–B(1)–C(21)	25.8	30.6	C(12)–C(7)–C(6)	106.9	107.5(2)
C(12)–N(1)–B(1)–C(30)	–154.2	–150.5			
C(35)–C(30)–B(1)–N(1)	58.6	59.2	C(25)–B(1)–C(24)–S(1)	16.4	17.2
C(22)–C(21)–B(1)–N(1)	58.6	51.0	S(1)–C(21)–N(1)–C(12)	–57.2	38.0

Table 3. Comparison of [CAM-B3LYP/6-311G(d,p)] calculated data for optimized geometries of **1–3** and observed UV/Vis absorption maxima (in cyclohexane); calculated values of dipole moment of ground and excited states [Debye].

Compound	$\lambda_{\text{max}}$ (calcd.) [nm]	Oscillator strength ( $f$ ) (calcd.)	$\lambda_{\text{max}}$ (exp.) [nm]	$\Delta\lambda_{\text{max}}$ (calcd. – exp.) [nm]	Ground-state dipole moment [ $\mu_{\text{g}}$ ]	Excited-state dipole moment [ $\mu_{\text{e}}$ ]
<b>1</b>	288.0	0.31	324	–36	0.21	3.70
<b>2</b>	314.5	0.59	374	–59.5	0.83	12.61
<b>3</b> >	329.5	0.53	390	–60.5	0.21	9.93

tion an ensemble of rotational isomers exist, including planar geometries. Moreover, one should also consider the possibility that the calculations simply overestimate these energies.

In the case of compound **2**, the most intense absorption corresponding to the HOMO→LUMO transition is calculated at  $\lambda = 314.5$  nm and thus differs from the ex-

perimentally determined value ( $\lambda = 374$  nm) by 59.5 nm. For **3**, this lowest energy absorption is calculated at the longest wavelength ( $\lambda = 329.5$  nm) and differs from the experimental value ( $\lambda = 390$  nm) by 60.5 nm. The computed HOMO→LUMO transition of **3** is thus red-shifted by 41.5 nm or 15 nm in comparison to **1** or **2**, respectively.

Table 4. [CAM-B3LYP/6-311G(d,p)] calculated MO energies  $\epsilon^{\text{KS}}$  (LUMO+2, LUMO+1, LUMO, HOMO, HOMO-1, HOMO-2, HOMO-LUMO gaps) and first four  $\Delta\text{SCF/TDDFT}$  ionization energies of **1**, **2**, and **3**. Contour values are plotted at  $\pm(0.04 \text{ e/bohr}^3)^{1/2}$ .



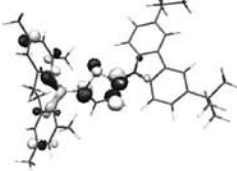
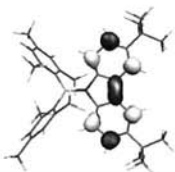
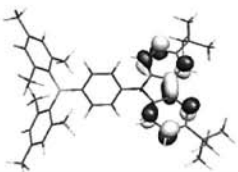
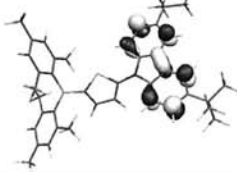

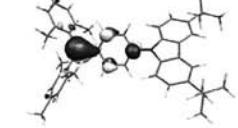
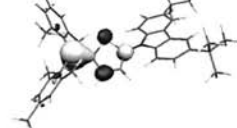
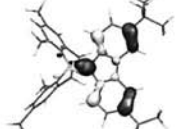
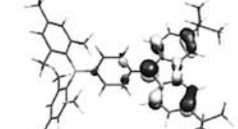
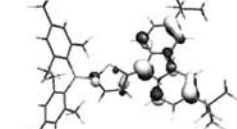


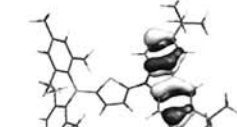


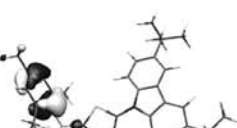
	<b>1</b>	<b>2</b>	<b>3</b>
LUMO+2 [eV]	0.927 $\pi^*$ (Mes) 	0.676 $\pi^*$ (phenyl) 	0.844 $\pi^*$ (crb, Mes) 
LUMO+1 [eV]	0.295 $\pi^*$ (crb) 	0.260 $\pi^*$ (crb) 	0.186 $\pi^*$ (crb) 
LUMO [eV]	-0.185 $2p_z^*$ 	-0.751 $2p_z^*$ (phenyl) 	-0.817 $2p_z^*$ (thioph) 
HOMO [eV]	-7.065 $\pi_1$ (crb) 	-6.730 $\pi_1$ (crb) 	-6.807 $\pi_1$ (crb) 
HOMO-1 [eV]	-7.149 $\pi_2$ (crb) 	-7.154 $\pi_2$ (crb) 	-7.231 $\pi_2$ (crb) 
HOMO-2 [eV]	-7.750 $\pi_3$ (Mes) 	-7.700 $\pi_3$ (Mes) 	-7.692 $\pi_3$ (Mes) 
HOMO-LUMO gap [eV – nm]	6.880 – 180.4	5.979 – 207.6	5.990 – 207.2
$IE_1$ [eV]	7.258	6.907	6.984
$IE_2$ [eV]	7.498	7.562	7.628
$IE_3$ [eV]	8.103	8.181	8.147
$IE_4$ [eV]	8.166	8.224	8.188

Table 4 displays the [CAM-B3LYP/6-311G(d,p)] calculated MO energies (LUMO, HOMO, HOMO–1) of **1–3**, as well as the HOMO–LUMO gaps, and the four first  $\Delta\text{SCF}/\text{TDDFT}$  ionization energies. The LUMOs of **1–3** are located on the vacant  $2p_z$  orbital of the boron atom with  $\pi^*$ -orbital contributions of the phenyl (in **2**) or thiophene (in **3**) unit, whereas the HOMO and HOMO–1 energies correspond to  $\pi_1(\text{crb})$  and  $\pi_2(\text{crb})$ , respectively, and are located on the carbazole part in the three molecules.

The attachment of the electron-withdrawing dimesitylboryl group to the nitrogen atom of the carbazole led to the stabilization of its HOMO ( $\pi_1$ ,  $-7.01$  eV) by  $0.25$  eV. In contrast, the linkage of the benzodiazaborole ring was accompanied by a destabilization of  $0.38$  eV, reflecting the electron-releasing character of the B/N heterocycle. The introduction of the phenylene unit between the dimesitylboryl and the carbazole fragments effects a destabilization of the HOMO (in **2**) by  $0.34$  eV, whereas the thiophenediyl unit (in **3**) evokes only half this effect ( $0.16$  eV) with respect to the (carbazol-9-yl)dimesitylborane **1**. This destabilization is due to the +M effect of these two spacers.

The position of HOMO–1 is insensitive towards substitution and is only very slightly stabilized in **2** ( $0.005$  eV) and in **3** ( $0.082$  eV) in comparison with **1**. The HOMO–LUMO gap is significantly smaller in **2** ( $5.979$  eV –  $207.6$  nm) and in **3** ( $5.990$  eV –  $207.2$  nm) than in **1** ( $6.880$  eV –  $180.4$  nm). The most important difference in the calculated ionization energies ( $IE$ ) is noted for **1** and highlights the influence of the acceptor properties of the boron atom directly linked to the nitrogen atom of carbazole ( $IE = 7.258$  eV). The formal insertion of a phenylene or a thiophene unit into the B–N bond of **1** provides a lowering of the  $IE$  [ $6.907$  (**2**) and  $6.984$  eV (**3**)] due to the donating properties of these two rings. Deeper energy ionizations seem practically unperturbed by their environment.

## Conclusion

Dimesitylborane derivatives **1–3** with carbazol-9-yl, 4-(carbazol-9-yl)phenyl, and 5-(carbazol-9-yl)-2-thienyl substituents have been synthesized. Molecules **1** and **3** have nonplanar geometries in the crystalline phase, as evidenced by X-crystallography, as well as in the gas phase, according to DFT calculations. In the UV/Vis spectra the low energy bands at  $\lambda = 324$  (**1**),  $374$  (**2**), and  $390$  nm (**3**) are assigned to HOMO→LUMO charge-transfer transitions, whereby the HOMOs are located at the carbazolyl part of the molecules. The LUMOs are mainly represented by the vacant  $2p_z$  orbital of the boron atom with  $\pi^*$ -orbital contributions of the phenyl or thiophene unit in **2** or **3**, respectively. Obviously, the replacement of the  $\pi$ -electron-donating 1,3,2-benzodiazaborolyl substituent by the efficient  $\pi$ -accepting dimesitylboryl group led to a significant change in the nature of the frontier orbitals. In the *N*-(benzodiazaborolyl)carbazole **4**, the HOMO and LUMO are located on the carbazole part of the molecule with no participation of the boron-containing moiety. In **1**, however, the LUMO is mainly represented by the  $2p_z$  orbital of the boryl group, whereas the HOMO remains on the carbazole part.

represented by the  $2p_z$  orbital of the boryl group, whereas the HOMO remains on the carbazole part.

The different nature of the dimesitylboryl and the 1,3,2-benzodiazaborolyl substituents is substantiated by the values of the HOMO energies of the free carbazole ( $-7.01$  eV), compound **1** ( $-7.26$  eV), and the 2-(carbazol-9-yl)-1,3,2-benzodiazaborole **4a** ( $-6.62$  eV). Destabilization of the HOMO energy of **1** was effected by the insertion of a phenylene or thiophene spacer into the B–N bond yielding HOMO energies of  $-6.73$  (in **2**) and  $-6.81$  eV (in **3**).

The lack of significant solvatochromism in the ground states of **1–3** was confirmed by the low calculated dipole moments ( $0.21$ – $0.83$  D). The fluorescence spectra of **1–3** (in cyclohexane) display bands at  $\lambda = 450$  (**1**),  $394$  (**2**), and  $414$  nm (**3**) connected with Stokes shifts of  $9000$ ,  $1400$ , and  $1600$   $\text{cm}^{-1}$ , respectively. Significant redshifts of the emission bands in polar solvents (THF,  $\text{CH}_2\text{Cl}_2$ ) are in line with significant polarities in the excited states, as also documented by calculated dipole moments of  $3.70$  (**1**),  $12.61$  (**2**), and  $9.93$  D (**3**).

Thus, benzodiazaborolyl and dimesitylboryl groups are contrasting building blocks in  $\pi$ -conjugated organic molecules. The idea to place both on the ends of push–pull molecules is challenging. Attempts to impose  $\pi$ -acceptor properties on the benzodiazaborole core involve the introduction of fluorinated aryl substituents at the nitrogen atoms of the molecules.

## Experimental Section

**General:** All manipulations were performed under dry, oxygen-free argon by using Schlenk techniques. All solvents were dried by standard methods and freshly distilled prior to use. The compounds 2-bromo-1,3-diethyl-1,3,2-benzodiazaborole,<sup>[22]</sup> fluorodimesitylborane,<sup>[12]</sup> 3,6-di-*tert*-butylcarbazole,<sup>[11]</sup> 3,6-di-*tert*-butyl-*N*-(2-thienyl)carbazole,<sup>[13]</sup> and 1-bromo-4-(3,6-di-*tert*-butylcarbazol-9-yl)-benzene<sup>[14]</sup> were prepared according to literature methods. NMR spectra were recorded at room temperature with a BrukerAM Avance DRX-500 spectrometer ( $^1\text{H}$ ,  $^{11}\text{B}$ ,  $^{13}\text{C}$ ) by using TMS and  $\text{BF}_3\cdot\text{OEt}_2$  as external standards. Mass spectra were taken with a VG autospec sector field mass spectrometer (Micromass). The UV/Vis spectra were recorded with a Thermo Evolution 300 UV/Vis spectrometer and the emission spectra with a Hitachi F-4500 fluorescence spectrometer.

**3,6-Di-*tert*-butyl-*N*-(dimesitylboryl)carbazole (**1**):** A solution of 3,6-di-*tert*-butylcarbazole ( $0.559$  g,  $2.0$  mmol) in *n*-pentane ( $30$  mL) was combined at  $20^\circ\text{C}$  with an equimolar amount of an *n*-butyllithium solution in *n*-hexane ( $1.6$  mL,  $1.25$  mmol). After stirring the mixture for  $1$  h, an *n*-pentane solution ( $10$  mL) of fluorodimesitylborane ( $0.540$  g,  $2.0$  mmol) was added. The slurry was stirred overnight, filtered, and the solvent and volatile components were removed from the filtrate. Purification of the residue was effected by column chromatography on silica with *n*-pentane. Product **1** ( $R_f = 0.25$ ) was crystallized from *n*-pentane to give  $0.753$  g ( $70\%$ ) of pure **1** as a colorless solid.  $^1\text{H}$  NMR ( $\text{CDCl}_3$ ):  $\delta = 1.42$  (s,  $18$  H, *t*Bu),  $2.07$  (s,  $12$  H, *o*- $\text{CH}_3$ ),  $2.36$  (s,  $6$  H, *p*- $\text{CH}_3$ ),  $6.84$  (m,  $6$  H, mesityl-H and *t*BuCCH=CH),  $7.13$  (dd,  $J = 1.7, 8.8$  Hz,  $2$  H, *t*BuCCH=CH),  $7.98$  (d,  $J = 1.7$  Hz,  $2$  H, *t*BuCCHC) ppm.  $^{13}\text{C}\{^1\text{H}\}$  NMR ( $\text{CDCl}_3$ ):  $\delta = 21.3$  (s, *p*- $\text{CH}_3$ ),  $21.9$  (s, *o*- $\text{CH}_3$ ),  $31.8$  [s, C-( $\text{CH}_3$ ) $_3$ ],  $34.6$  [s, C( $\text{CH}_3$ ) $_3$ ],  $114.9$  (s, *t*BuCCHCH),  $115.4$  (s,



*t*BuCCHC), 123.8 (s, *t*BuCCHCH), 128.6 [s, BCCCHC(CH<sub>3</sub>)], 128.1, 141.0, 141.6 (3 s, *t*BuCCHCC), 138.8, 145.5 [2 s, BCC(CH<sub>3</sub>)CHC(CH<sub>3</sub>)] ppm. <sup>1</sup>B{<sup>1</sup>H}NMR (CDCl<sub>3</sub>): δ = 51.0 ppm. IR (ATP, diamond):  $\tilde{\nu}$  = 3027 (w), 2949 (s), 2918 (s), 1606 (m), 1690 (m), 1467 (s), 1392 (s), 1298 (m), 850 (s), 818 (s) cm<sup>-1</sup>. MS/EI: *m/z* (%) = 527.4 (100) [M]<sup>+</sup>, 512.4 (41) [M – CH<sub>3</sub>]<sup>+</sup>, 249.2 (68) [B – Mes<sub>2</sub>]<sup>+</sup>. C<sub>38</sub>H<sub>46</sub>BN (527.61): calcd. C 86.51, H 8.79, N 2.65; found C 86.50, H 9.01, N 2.40.

**[4-(3,6-Di-*tert*-butylcarbazol-9-yl)phenyl]dimesitylborene (2):** A solution of *n*-butyllithium in *n*-hexane (1.6 M, 1.70 mL, 2.70 mmol) was added dropwise to a chilled solution (–78 °C) of *N*-(4-bromophenyl)-3,6-di-*tert*-butylcarbazole (1.20 g, 2.70 mmol) in diethyl ether (50 mL). After warming the mixture to –20 °C, a solution of fluorodimesitylborene (0.72 g, 2.70 mmol) in *n*-pentane (10 mL) was added. The reaction mixture was slowly warmed to room temperature and stirred overnight. Water (10 mL) was added and the separated organic layer was dried with Na<sub>2</sub>SO<sub>4</sub>. The solvent was removed in vacuo from a colorless solid residue, which was subsequently crystallized from *n*-hexane (25 mL). Yield: 0.97 g (59%) of **2** as colorless crystals. <sup>1</sup>H NMR (CDCl<sub>3</sub>): δ = 1.59 (s, 18 H, *t*Bu), 2.22 (s, 12 H, *o*-CH<sub>3</sub>), 2.44 (s, 6 H, *p*-CH<sub>3</sub>), 6.98 (s, 4 H, mesityl-H), 7.59 (s, 4 H, *t*BuCCHCHC), 7.68 (d, *J* = 8 Hz, 2 H, NCCHCHCB), 7.84 (d, *J* = 8 Hz, 2 H, NCCHCHCB), 8.27 (s, 2 H, *t*BuCCHC) ppm. <sup>13</sup>C{<sup>1</sup>H}NMR (CDCl<sub>3</sub>): δ = 21.2 (s, *p*-CH<sub>3</sub>), 23.5 (s, *o*-CH<sub>3</sub>), 31.9 [s, C(CH<sub>3</sub>)<sub>3</sub>], 34.7 [s, C(CH<sub>3</sub>)<sub>3</sub>], 109.4 (s, *t*BuCCHCHC), 116.3 (s, *t*BuCCHC), 123.7 (s, *t*BuCCHCHC), 125.3 (s, NCCHCHCB), 128.2 [s, BCCCHC(CH<sub>3</sub>)], 137.9 (s, NCCHCHCB) 123.7, 138.8, 143.2 (3 s, *t*BuCCHCC), 138.7, 140.8 [2 s, BCC(CH<sub>3</sub>)CHC(CH<sub>3</sub>)], 141.4 (s, NCCHCHCB), 141.6 [s, BCC(CH<sub>3</sub>)CH], 143.9 (s, NCCHCHCB) ppm. <sup>1</sup>B{<sup>1</sup>H}NMR (CDCl<sub>3</sub>): δ = 71.3 ppm. IR (ATP, diamond):  $\tilde{\nu}$  = 3018 (w), 2959 (s), 1605 (m), 1487 (m), 1470 (s), 1390 (s), 1218 (m), 831 (s), 802 (s) cm<sup>-1</sup>. MS/EI: *m/z* (%) = 603.4 (100) [M]<sup>+</sup>, 588.0 (44) [M – CH<sub>3</sub>]<sup>+</sup>. C<sub>44</sub>H<sub>50</sub>BN (603.71): calcd. C 87.54, H 8.35, N 2.32; found C 87.29, H 8.36, N 2.43.

**5-(3,6-Di-*tert*-butylcarbazol-9-yl)-2-(dimesitylboryl)thiophene (3):** An *n*-hexane solution of *n*-butyllithium (1.6 M, 2.1 mL, 3.4 mmol) was added dropwise at room temperature to a well-stirred solution of 2-(3,6-di-*tert*-butylcarbazol-9-yl)thiophene (1.2 g, 3.3 mmol) in diethyl ether (50 mL). After 1 h, an *n*-pentane solution (10 mL) of fluorodimesitylborene (0.9 g, 3.3 mmol) was added, and stirring was continued overnight. The slurry was combined with water (10 mL). The organic layer was separated and dried with Na<sub>2</sub>SO<sub>4</sub>. The solvent and volatile components were removed in vacuo, and the yellow, solid residue was recrystallized from *n*-hexane (40 mL). Yield: 1.3 g (66%) of colorless crystalline **3**. <sup>1</sup>H NMR (CDCl<sub>3</sub>): δ = 1.52 (s, 18 H, *t*Bu), 2.28 (s, 12 H, *o*-CH<sub>3</sub>), 2.38 (s, 6 H, *p*-CH<sub>3</sub>), 6.92 (s, 4 H, mesityl-H), 7.37 (d, *J* = 3.8 Hz, 1 H, NCCHCHCS), 7.56 (dd, *J* = 1.7, 8.5 Hz, 2 H, *t*BuCCHCHC), 7.58 (d, *J* = 3.8 Hz, 1 H, NCCHCHCS), 7.70 (d, *J* = 8.5 Hz, 2 H, *t*BuCCHCHC), 8.15 (d, *J* = 1.7 Hz, 2 H, *t*BuCCHC) ppm. <sup>13</sup>C{<sup>1</sup>H}NMR (CDCl<sub>3</sub>): δ = 21.2 (s, *p*-CH<sub>3</sub>), 23.5 (s, *o*-CH<sub>3</sub>), 31.9 [s, C(CH<sub>3</sub>)<sub>3</sub>], 34.7 [s, C(CH<sub>3</sub>)<sub>3</sub>], 110.0 (s, *t*BuCCHCHC), 116.2 (s, *t*BuCCHC), 123.5 (s, NCCHCHCS), 124.0 (s, *t*BuCCHCHC), 128.2 [s, BCCCHC(CH<sub>3</sub>)], 140.3 (s, NCCHCHCS) 123.9, 139.0, 141.0 (3 s, *t*BuCCHCC), 144.1, 145.7 [2 s, BCC(CH<sub>3</sub>)CHC(CH<sub>3</sub>)] 152.0 (s, NCCHCHCS) ppm. <sup>1</sup>B{<sup>1</sup>H}NMR (CDCl<sub>3</sub>): δ = 64.9 ppm. IR (ATP, diamond):  $\tilde{\nu}$  = 2950 (s), 1605 (m), 1518 (m), 1487 (m), 1430 (s), 1363 (s), 1224 (m), 844 (s), 820 (s), 713 (s), 610 (s) cm<sup>-1</sup>. MS/EI: *m/z* (%) = 609.5 (100) [M]<sup>+</sup>, 594.4 (44) [M – CH<sub>3</sub>]<sup>+</sup>, 248.2 (20) [BMes<sub>2</sub>]<sup>+</sup>. C<sub>42</sub>H<sub>48</sub>BNS (609.73): calcd. C 82.74, H 7.94, N 2.30; found C 82.28, H 7.93, N 2.25.

**2-[4-(3,6-Di-*tert*-butylcarbazol-9-yl)phenyl]-1,3-diethyl-1,3,2-benzodiazaborole (5):** Samples of 1-bromo-4-(3,6-di-*tert*-butylcarbazol-9-yl)benzene (1.00 g, 2.3 mmol) and 2-bromo-1,3-diethyl-1,3,2-benzodiazaborole (0.65 g, 2.6 mmol) were added to a mixture of magnesium metal (0.20 g, 8.2 mmol) and LiCl (0.13 g, 3.0 mmol) in THF (30 mL). The resulting mixture was heated under reflux for 18 h, and the volatile components were removed in vacuo. The residue was triturated with *n*-pentane (30 mL). The filtered solution was stored at –20 °C whereby colorless crystals of **5** separated. Yield: 0.82 g (68%). <sup>1</sup>H NMR (CDCl<sub>3</sub>): δ = 1.45 (t, *J* = 7.1 Hz, 6 H, NCH<sub>2</sub>CH<sub>3</sub>), 1.53 [s, 18 H, C(CH<sub>3</sub>)<sub>3</sub>], 3.94 (q, *J* = 7.1 Hz, 4 H, NCH<sub>2</sub>CH<sub>3</sub>), 7.13 (m, 2 H, CH=CHCH=CH), 7.21 (m, 2 H, CH=CHCH=CH), 7.53 (m, 4 H, *t*BuCCHC, *t*BuCCHCH), 7.71 (d, *J* = 8.5 Hz, NCCHCHCB), 7.82 (d, *J* = 8.5 Hz, NCCHCHCB), 8.2 (s, 2 H, *t*BuCCHCHC) ppm. <sup>13</sup>C{<sup>1</sup>H}NMR (CDCl<sub>3</sub>): δ = 16.3 (s, NCH<sub>2</sub>CH<sub>3</sub>) 32.0 [s, C(CH<sub>3</sub>)<sub>3</sub>], 34.7 [s, C(CH<sub>3</sub>)<sub>3</sub>], 37.7 (s, NCH<sub>2</sub>CH<sub>3</sub>), 108.9 (s, CH=CHCH=CH), 109.3 (s, *t*BuCCHCHC), 116.2 (s, *t*BuCCHC), 118.8 (s, CH=CHCH=CH), 123.6 (s, *t*BuCCHCHC), 126.0 (s, NCCHCHCB), 134.8 (s, NCCHCHCB), 137.1 (s, N<sub>2</sub>C<sub>2</sub>), 138.5 (s, NCCHCHCB), 123.4, 139.1, 142.9 (3 s, *t*BuCCHCC) ppm. <sup>1</sup>B{<sup>1</sup>H}NMR (CDCl<sub>3</sub>): δ = 28.6 ppm. IR (ATP, diamond):  $\tilde{\nu}$  = 3034 (w), 2956 (s), 2926 (m), 1600 (s), 1519 (s), 1470 (s), 1401 (s), 1371 (s), 1263 (m), 1233 (s), 1045 (m), 875 (w), 809 (s), 667 (m) cm<sup>-1</sup>. MS/EI: *m/z* (%) = 527.4 (100) [M]<sup>+</sup>, 512.4 (69) [M – CH<sub>3</sub>]<sup>+</sup>. C<sub>42</sub>H<sub>48</sub>BNS (527.57): calcd. C 81.96, H 8.02, N 7.96; found C 81.16, H 8.37, N 7.57.

**X-ray Crystallography:** Single crystals of **1** and **2** were coated with a layer of hydrocarbon oil, attached to a glass fiber, and cooled to 100 K for data collection. Crystallographic data were collected with a Nonius Kappa CCD diffractometer with Mo-*K*<sub>α</sub> radiation (graphite monochromator), λ = 0.71073 Å. Crystallographic programs used for the structure solution and refinement were from SHELXL-97.<sup>[23]</sup> The structure was solved by direct methods and was refined by using full-matrix least squares on *F*<sup>2</sup> of all unique reflections with anisotropic thermal parameters for all non-hydrogen atoms. Hydrogen atoms were included at calculated positions with *U*(H) = 1.2 *U*<sub>eq</sub> for CH<sub>2</sub> groups and *U*(H) = 1.5 *U*<sub>eq</sub> for CH<sub>3</sub> groups. Crystal data for the compounds are listed in Table 5. CCDC-811962 (for **1**) and -811963 (for **3**) contain the supplementary crystallographic data for this paper. These data can be obtained free of charge from Cambridge Crystallographic Data Centre via [www.ccd.cam.ac.uk/data\\_request/cif](http://www.ccd.cam.ac.uk/data_request/cif) or as ESI.

**Computational Methods:** All calculations were performed by using the Gaussian 09<sup>[25]</sup> program package with the 6-311G(d,p) basis set. DFT has been shown to predict various molecular properties successfully.<sup>[26]</sup> All geometry optimizations were carried out with the CAM-B3LYP<sup>[27]</sup> functional and were followed by frequency calculations to verify that the stationary points obtained are true energy minima. Ionization energies (*IE*) were calculated by using the CAM-B3LYP functional (which is particularly well suited for ionization energy evaluations; see for example ref.<sup>[9]</sup>) with ΔSCF/TD-DFT, which means that separate SCF calculations were performed to optimize the orbitals of the ground state and the appropriate ionic state (*IE* = *E*<sub>cation</sub> – *E*<sub>neutral</sub>). The advantages of the most frequently employed ΔSCF/TD-DFT method of calculations of the first ionization energies have been demonstrated previously.<sup>[28]</sup> The TD-DFT<sup>[29]</sup> approach provides a first principal method for the calculation of excitation energies within a density functional context taking into account the low-lying ion calculated by ΔSCF method.

**Supporting Information** (see footnote on the first page of this article): Tables of atomic coordinates for [CAM-B3LYP/6-311G(d,p)]

Table 5. Crystallographic data of **1** and **3**.

	<b>1</b>	<b>3</b>
Empirical formula	C <sub>38</sub> H <sub>46</sub> BN·0.5C <sub>5</sub> H <sub>12</sub>	C <sub>42</sub> H <sub>48</sub> BNS
<i>M<sub>r</sub></i> [g mol <sup>-1</sup> ]	563.64	609.68
Crystal dimension [mm]	0.22 × 0.14 × 0.12	0.30 × 0.13 × 0.10
Crystal system	monoclinic	monoclinic
Space group	<i>C</i> 2/ <i>c</i>	<i>P</i> 2 <sub>1</sub> / <i>c</i>
<i>a</i> [Å]	30.4874(11)	13.9022(6)
<i>b</i> [Å]	20.1111(10)	18.3085(9)
<i>c</i> [Å]	11.7183(3)	13.9814(5)
$\beta$ [°]	98.155(2)	96.800(2)
<i>V</i> [Å <sup>3</sup> ]	7112.2(5)	3533.6(2)
<i>Z</i>	8	4
$\rho_{\text{calcd.}}$ [g cm <sup>-3</sup> ]	1.053	1.146
$\mu$ [mm <sup>-1</sup> ]	0.059	0.121
<i>F</i> (000)	2456	1312
$\theta$ [°]	3.0–25.0	3.0–25.0
No. refl. collected	19755	26962
No. refl. unique	6252	6136
<i>R</i> (int)	0.047	0.080
No. refl. [ <i>I</i> > 2σ( <i>I</i> )]	4821	4136
Refined parameter	372	430
GOF	0.975	1.007
<i>R<sub>F</sub></i> [ <i>I</i> > 2σ( <i>I</i> )]	0.0604	0.0480
<i>wR<sub>F2</sub></i> (all data)	0.1739	0.1227
$\Delta\rho_{\text{max/min}}$ [e Å <sup>-3</sup> ]	0.629/–0.390	0.205/–0.282
Remarks	0.5 pentane molecules were disordered near an inversion center and could not be satisfactorily refined. The routine squeeze of Platon <sup>[24]</sup> was used to remove the electron density of the solvent, but the empirical formula includes the solvent for further calculations. Disorder of C(14), C(15), and C(16) on two positions (70:30).	Disorder of <i>tert</i> -butyl group C(18), C(19), and C(20) on three positions (42:30:28). One idealized disordered methyl group [C(32)].

optimized geometries, values of total energies, ionization energies (*IE*s) and UV/Vis spectra of **1**–**3**.

- [1] a) C. D. Entwistle, T. B. Marder, *Angew. Chem.* **2002**, *114*, 3051–3056; *Angew. Chem. Int. Ed.* **2002**, *41*, 2927–2931; b) C. D. Entwistle, T. B. Marder, *Chem. Mater.* **2004**, *16*, 4574–4585; c) S. Yamaguchi, A. Wakamiya, *Pure Appl. Chem.* **2006**, *78*, 1413–1424; d) F. Jäkle, *Coord. Chem. Rev.* **2006**, *250*, 1107–1121.
- [2] a) Z. Yuan, N. J. Taylor, T. B. Marder, I. D. Williams, S. K. Kurtz, L.-T. Cheng, *J. Chem. Soc., Chem. Commun.* **1990**, 1489–1492; b) Z. Yuan, N. J. Taylor, T. B. Marder, I. D. Williams, S. K. Kurtz, L.-T. Cheng, *Organic Materials for Non-linear Optic II* (Eds.: R. A. Hann, D. Bloor), RCS, Cambridge, **1991**, p. 190; c) M. Lequan, R. M. Lequan, K. Chane-Ching, *J. Mater. Chem.* **1991**, *1*, 997–999; d) M. Lequan, R. M. Lequan, K. Chane-Ching, M. Barzoukas, A. Fort, H. Lahoucine, G. Bravic, J. Chasseau, J. Gaultier, *J. Mater. Chem.* **1992**, *2*, 719–725; e) M. Lequan, R. M. Lequan, K. Chane-Ching, A.-C. Callier, M. Barzoukas, A. Fort, *Adv. Mater. Opt. Electron.* **1992**, *1*, 243–247; f) Z. Yuan, N. J. Taylor, Y. Sun, T. B. Marder, I. D. Williams, L.-T. Cheng, *J. Organomet. Chem.* **1993**, *449*, 27–37; g) C. Branger, M. Lequan, R. M. Lequan, M. Barzoukas, A. Fort, *J. Mater. Chem.* **1996**, *6*, 555–558; h) Z. Yuan, N. J. Taylor, R. Ramachandran, T. B. Marder, *Appl. Organomet. Chem.* **1996**, *10*, 305–316; i) Z. Yuan, J. C. Collings, N. J. Taylor, T. B. Marder, C. Jardin, J.-F. Halet, *J. Solid State Chem.* **2000**, *154*, 5–12; j) Y. Liu, X. Xu, F. Zheng, Y. Cui, *Angew. Chem.* **2008**, *120*, 4614–4617; *Angew. Chem. Int. Ed.* **2008**, *47*, 4538–4541.
- [3] Z. Yuan, C. D. Entwistle, J. C. Collings, D. Albesa-Jove, A. S. Bahanov, J. A. K. Howard, H. M. Kaiser, D. E. Kaufmann, S.-

- Y. Poon, W.-Y. Wong, C. Jardin, S. Fatallah, A. Boucekkine, J.-F. Halet, T. B. Marder, *Chem. Eur. J.* **2006**, *12*, 2758–2771.
- [4] a) Z.-Q. Liu, Q. Fang, D. Wang, G. Xue, W.-T. Yu, Z.-S. Shao, M.-H. Jiang, *Chem. Commun.* **2002**, 2900–2901; b) Z.-Q. Liu, Q. Fang, D. Wang, D.-X. Cao, G. Xue, W.-T. Yu, H. Lei, *Chem. Eur. J.* **2003**, *9*, 5074–5084; c) D.-X. Cao, Z.-Q. Liu, Q. Fang, G.-B. Xu, G. Xue, G.-Q. Liu, W.-T. Yu, *J. Organomet. Chem.* **2004**, *689*, 2201–2206; d) Z.-Q. Liu, Q. Fang, D.-X. Cao, D. Wang, G.-B. Xu, *Org. Lett.* **2004**, *6*, 2933–2936; e) Z.-Q. Liu, M. Shi, F.-Y. Li, Q. Fang, Z.-H. Clen, T. Yi, C.-H. Huang, *Org. Lett.* **2005**, *7*, 5481–5484; f) M. Charlot, L. Porrès, C. D. Entwistle, A. Beeby, T. B. Marder, M. Blanchard-Desce, *Phys. Chem. Chem. Phys.* **2005**, *7*, 600–606; g) L. Porrès, M. Charlot, C. D. Entwistle, A. Beeby, T. B. Marder, M. Blanchard-Desce, *Proc. SPIE Int. Soc. Opt. Eng.* **2005**, *5934*, 92; h) D.-X. Cao, Z.-Q. Liu, G.-Z. Li, G.-Q. Liu, G.-H. Zhang, *J. Mol. Struct.* **2008**, *874*, 46–50; i) J. C. Collings, S.-Y. Poon, G. Le Droumarguet, M. Charlot, C. Katan, L.-O. Pålsson, A. Beeby, J. A. Mosely, H. M. Kaiser, D. Kaufmann, W.-Y. Wong, M. Blanchard-Desce, T. B. Marder, *Chem. Eur. J.* **2009**, *15*, 198–208.
- [5] a) T. Noda, Y. Shirota, *J. Am. Chem. Soc.* **1998**, *120*, 9714–9715; b) T. Noda, H. Ogawa, Y. Shirota, *Adv. Mater.* **1999**, *11*, 283–285; c) T. Noda, Y. Shirota, *J. Lumin.* **2000**, *87*–89, 1168–1170; d) Y. Shirota, M. Kinoshita, T. Noda, K. Okumoto, T. Ohara, *J. Am. Chem. Soc.* **2000**, *122*, 11021–11022; e) M. Kinoshita, N. Fujii, T. Tsukaki, Y. Shirota, *Synth. Met.* **2001**, *121*, 1571–1572; f) H. Doi, M. Kinoshita, K. Okumoto, Y. Shirota, *Chem. Mater.* **2003**, *15*, 1080–1089; g) W.-L. Jia, D.-R. Bai, T. McCormick, Q.-D. Liu, M. Motala, R.-Y. Wang, C. Seward, Y. Tao, S. Wang, *Chem. Eur. J.* **2004**, *10*, 994–1006; h) W.-L. Jia, D. Feng, D.-R. Bai, Z. H. Lu, S. Wang, G. Vamvounis, *Chem. Mater.* **2005**, *17*, 164–170; i) W.-L. Jia, M. J. Moran, Y.-Y. Yuan, Z. H. Lu, S. Wang, *J. Mater. Chem.* **2005**, *15*, 3326–

- 3333; j) M. Mazzeo, V. Vitale, F. Della Sala, M. Anni, G. Barbarella, L. Favaretto, G. Sotgui, R. Cingolani, G. Gigli, *Adv. Mater.* **2005**, *17*, 34–39; k) G.-J. Zhou, G.-L. Ho, W.-Y. Wong, Q. Wang, D.-G. Ma, L.-X. Wang, Z.-Y. Lin, T. B. Marder, A. Beeby, *Adv. Funct. Mater.* **2008**, *18*, 499–511.
- [6] a) For reviews on 1,3,2-diazaboroles, see: L. Weber, *Coord. Chem. Rev.* **2001**, *215*, 39–77; b) L. Weber, *Coord. Chem. Rev.* **2008**, *252*, 1–31; c) M. Yamashita, K. Nozaki, *Pure Appl. Chem.* **2008**, *80*, 1187–1194; d) M. Yamashita, K. Nozaki, *Bull. Chem. Soc. Jpn.* **2008**, *81*, 1377–1392.
- [7] a) L. Weber, V. Werner, I. Domke, H.-G. Stammer, B. Neumann, *Dalton Trans.* **2006**, 3777–3784; b) L. Weber, V. Werner, M. A. Fox, T. B. Marder, S. Schwedler, A. Brockhinke, H.-G. Stammer, B. Neumann, *Dalton Trans.* **2009**, 1339–1351.
- [8] L. Weber, V. Werner, M. A. Fox, T. B. Marder, S. Schwedler, A. Brockhinke, H.-G. Stammer, B. Neumann, *Dalton Trans.* **2009**, 2823–2831.
- [9] A. Chrostowska, M. Maciejczyk, A. Dargelos, P. Baylère, L. Weber, V. Werner, D. Eickhoff, H. G. Stammer, B. Neumann, *Organometallics* **2010**, *29*, 5192–5198.
- [10] L. Weber, J. Halama, V. Werner, K. Hanke, L. Böhl, A. Chrostowska, A. Dargelos, M. Maciejczyk, A.-L. Raza, H.-G. Stammer, B. Neumann, *Eur. J. Inorg. Chem.* **2010**, 5416–5425.
- [11] T. Xu, R. Lu, X. Lin, X. Zheng, X. Qin, Y. Zhao, *Org. Lett.* **2007**, *9*, 797–800.
- [12] A. Pelter, K. Smith, H. C. Brown, *Borane Reagents*, Academic Press, London **1988**, p. 428.
- [13] A. Hameurlaine, W. Dahaen, *Tetrahedron Lett.* **2003**, *44*, 957–959.
- [14] Y. Lin, M. Nishiura, Y. Wang, Z. Hou, *J. Am. Chem. Soc.* **2006**, *128*, 5592–5593.
- [15] P. Paetzold, *Adv. Inorg. Chem.* **1987**, *31*, 123–170.
- [16] D. J. Brauer, H. Bürger, F. Dörrenbach, G. Pawelke, W. Weuter, *J. Organomet. Chem.* **1989**, *378*, 125–137.
- [17] D. X. Cao, Z. Q. Liu, Y. Fang, G. B. Xu, G. Xue, G. Q. Liu, W. T. Yu, *J. Organomet. Chem.* **2004**, *689*, 2201–2206.
- [18] S.-B. Zhao, P. Wucher, Z. M. Hudson, T. M. McCormick, X.-Y. Liu, S. Wang, X.-D. Feng, Z.-H. Lu, *Organometallics* **2008**, *27*, 6446–6456.
- [19] R. Stahl, C. Lambert, C. Kaiser, R. Wortmann, R. Jakober, *Chem. Eur. J.* **2006**, *12*, 2358–2370.
- [20] G. Meshulam, G. Berkovic, Z. Kotler, A. Ben-Asuly, R. Mazor, L. Shapiro, V. Khodorkovsky, *Synth. Met.* **2000**, *115*, 219–223.
- [21] A. Kapturkiewicz, J. Herbich, J. Kapiuk, J. Nowacki, *J. Phys. Chem. A* **1997**, *101*, 2332–2344.
- [22] L. Weber, H. B. Wartig, H.-G. Stammer, B. Neumann, *Z. Anorg. Allg. Chem.* **2001**, *627*, 2663–2668.
- [23] G. M. Sheldrick, *SHELX-97, Program for Crystal Structure Refinement*, University of Göttingen, **1997**.
- [24] A. L. Spek, *PLATON, A Multipurpose Crystallographic Tool*, Utrecht University, Utrecht, The Netherlands, **2008**.
- [25] M. J. Frisch, G. W. Trucks, H. B. Schlegel, G. E. Scuseria, M. A. Robb, J. R. Cheeseman, J. A. Montgomery Jr., T. Vreven, K. N. Kudin, J. C. Burant, J. M. Millam, S. S. Iyengar, J. Tomasi, V. Barone, B. Mennucci, M. Cossi, G. Scalmani, N. Rega, G. A. Petersson, H. Nakatsuji, M. Hada, M. Ehara, K. Toyota, R. Fukuda, J. Hasegawa, M. Ishida, T. Nakajima, Y. Honda, O. Kitao, H. Nakai, M. Klene, X. Li, J. E. Knox, H. P. Hratchian, J. B. Cross, V. Bakken, C. Adamo, J. Jaramillo, R. Gomperts, R. E. Stratmann, O. Yazyev, A. J. Austin, R. Cammi, C. Pomelli, J. W. Ochterski, P. Y. Ayala, K. Morokuma, G. A. Voth, P. Salvador, J. J. Dannenberg, V. G. Zakrzewski, S. Dapprich, A. D. Daniels, M. C. Strain, O. Farkas, D. K. Malick, A. D. Rabuck, K. Raghavachari, J. B. Foresman, J. V. Ortiz, Q. Cui, A. G. Baboul, S. Clifford, J. Cioslowski, B. B. Stefanov, G. Liu, A. Liashenko, P. Piskorz, I. Komaromi, R. L. Martin, D. J. Fox, T. Keith, M. A. Al-Laham, C. Y. Peng, A. Nanayakkara, M. Challacombe, P. M. W. Gill, B. Johnson, W. Chen, M. W. Wong, C. Gonzalez, J. A. Pople, *Gaussian 03, Revision E.01*, Gaussian, Inc., Wallingford, CT, USA, **2007**.
- [26] a) R. G. Parr, W. Yang, *Functional Theory of Atoms and Molecules*, Oxford University Press, New York, **1989**; b) M. J. Frisch, G. W. Trucks, J. R. Cheeseman, in *Recent Development and Applications of Modern Density Functional Theory, Theoretical and Computational Chemistry* (Ed.: J. M. Seminario), Elsevier, Amsterdam, Lausanne, New York, Oxford, Shannon, Tokyo, **1996**, vol. 4, pp. 679–707.
- [27] a) A. D. Becke, *Phys. Rev.* **1988**, *38*, 3098–3100; b) A. D. Becke, *J. Chem. Phys.* **1993**, *98*, 5648–5652; c) C. Lee, W. Yang, R. G. Parr, *Phys. Rev. B* **1988**, *37*, 785–789.
- [28] a) S. Joantéguy, G. Pfister-Guillouzo, H. Chermette, *J. Phys. Chem. B J. Phys. Chem.* **1999**, *103*, 3505–3511; b) A. Chrostowska, K. Miqueu, G. Pfister-Guillouzo, E. Briard, J. Levillain, J.-L. Ripoll, *J. Mol. Spectrosc.* **2001**, *205*, 323–330; c) R. Bartnik, P. Baylère, A. Chrostowska, A. Galindo, S. Lesniak, G. Pfister-Guillouzo, *Eur. J. Org. Chem.* **2003**, 2475–2479.
- [29] a) R. E. Stratmann, G. E. Scuseria, M. J. Frisch, *J. Chem. Phys.* **1998**, *109*, 8218–8224; b) M. E. Casida, C. Jamorski, K. C. Casida, D. R. Salahub, *J. Chem. Phys.* **1998**, *108*, 4439–4449; c) V. Lemierre, A. Chrostowska, A. Dargelos, H. Chermette, *J. Phys. Chem. A* **2005**, *109*, 8348–8355.

Received: February 4, 2011  
Published Online: June 6, 2011